

Anchoring of FLT3 in the endoplasmic reticulum alters signaling quality

*Dirk Schmidt-Arras,¹ *Sylvia-Annette Böhmer,¹ Sina Koch,² Jörg P. Müller,¹ Lutz Blei,¹ Hauke Cornils,¹ Reinhard Bauer,¹ Sridhar Korasikha,¹ Christian Thiede,² and Frank-D. Böhmer¹

¹Institute of Molecular Cell Biology, Center for Molecular Biomedicine, Friedrich Schiller University Jena, Jena; and ²Medizinische Klinik und Poliklinik I, Universitätsklinikum Carl Gustav Carus der Technischen Universität, Dresden, Germany

The mechanism of cell transformation by Fms-like tyrosine kinase 3 (FLT3) in acute myeloid leukemia (AML) is incompletely understood. The most prevalent activated mutant FLT3 ITD exhibits an altered signaling quality, including strong activation of the STAT5 transcription factor. FLT3 ITD has also been found partially retained as a high-mannose precursor in an intracellular compartment. To analyze the role of intracellular retention of FLT3 for transformation, we

have generated FLT3 versions that are anchored in the perinuclear endoplasmic reticulum (ER) by appending an ER retention sequence containing a RRR (R3) motif. ER retention of R3, but not of corresponding A3 FLT3 versions, is shown by biochemical, fluorescence-activated cell sorting, and immunocytochemical analyses. ER anchoring reduced global autophosphorylation and diminished constitutive activation of ERK1/2 and AKT of the constitutively active FLT3

versions. ER anchoring was, however, associated with elevated signaling to STAT3. Transforming activity of the FLT3 D835Y mutant was suppressed by ER anchoring. In contrast, ER-anchored FLT3 ITD retained STAT5-activating capacity and was transforming in vitro and in vivo. The findings highlight another aspect of the different signaling quality of FLT3 ITD: it can transform cells from an intracellular location. (Blood. 2009;113:3568-3576)

Introduction

Mutations in the gene encoding the receptor tyrosine kinase FLT3 (fms-like tyrosine kinase 3) which lead to constitutive activation are among the most common molecular lesions found in acute myeloid leukemia (AML).¹ The most prevalent type of mutations result in an internal tandem duplication (ITD) of amino acid stretches in the juxtamembrane domain of FLT3.² These alterations are predicted to abrogate an inhibitory interaction of this domain with the kinase domain.³ FLT3 ITD is highly active and can transform myeloid cell lines in vitro,⁴ and transduction of primary mouse bone marrow with FLT3 ITD-encoding retroviruses results in a myeloproliferative disorder (MPD).^{5,6} Other activating mutations of FLT3 have also been found in AML, including point mutations in the activation loop and, recently, activating point mutations in the juxtamembrane domain^{7,8} and ITD mutations in the kinase domain.⁹ FLT3 ITD and other activated forms of FLT3 are therefore considered as a therapeutic target in AML, and the development of FLT3-inhibiting agents is actively pursued.^{10,11}

Wild-type FLT3 and mutants with amino acid substitutions in the activation loop on the one hand and FLT3 ITD versions on the other hand exhibit qualitative differences in signal transduction. Notably, although FLT3 ITD strongly and directly activates STAT5 and has also been reported to activate STAT3, ligand-activated wild-type FLT3 or FLT3 activation loop point mutants are comparatively weak STAT5 activators.^{4,6,12-15} These differences correlate with a different transforming potential: FLT3 ITD is more penetrant in inducing MPD in mice than FLT3 D835Y, the most common activated point mutant,⁶ suggesting that STAT5 and STAT5 target gene activation are particularly important for AML carcinogenesis.

The molecular reasons for the different signaling quality of FLT3 ITD are currently unknown. We have previously observed that FLT3 ITD-expressing cells contain elevated levels of an EndoH-sensitive, 130-kDa high-mannose form of the receptor, as opposed to the complex glycosylated 150-kDa form. Further analysis showed that FLT3 ITD is partially retained in an intracellular compartment, at least partially in the endoplasmic reticulum (ER), by a mechanism that depends on its kinase activity and autophosphorylation.¹⁶ Similar observations have recently been made for transforming mutants of c-Kit.¹⁷ These findings led us to speculate that signaling from an intracellular compartment may contribute to the altered signaling quality of FLT3 ITD and, potentially, to FLT3 activation and transformation. To test this hypothesis, we have generated FLT3 mutants by attaching an appropriate targeting sequence containing an RRR motif to the C-terminus of either wild-type FLT3 or the constitutively active FLT3 D835Y and FLT3 ITD. These mutants are largely retained in an underglycosylated state in the ER, whereas the corresponding control versions (AAA) mature normally. ER retention of wild-type FLT3 or of the D835Y elicits some activation of STAT1 and STAT3 but does not induce cytokine-independent growth. Moreover, constitutive signaling of FLT3 D835Y to Erk1/2 and AKT as well as its transforming capacity is suppressed. In contrast, ER-anchored FLT3 ITD can still activate STAT5 and partially retains transforming capacity. The data support that differential localization of FLT3 is associated with different signaling quality and that ER entrapment leads to a selective suppression of signaling pathways which mediate transformation by FLT3 D835Y but not of STAT5 activation by FLT3 ITD.

Submitted October 31, 2007; accepted January 14, 2009. Prepublished online as *Blood* First Edition paper, February 9, 2009; DOI 10.1182/blood-2007-10-121426.

*D.S.-A. and S.-A.B. contributed equally to this study.

The online version of this article contains a data supplement.

The publication costs of this article were defrayed in part by page charge payment. Therefore, and solely to indicate this fact, this article is hereby marked "advertisement" in accordance with 18 USC section 1734.

© 2009 by The American Society of Hematology

Methods

Antibodies

Polyclonal rabbit anti-FLT3 antibodies S18 and C20 were kindly provided by Lars Rönstrand (Wallenberg Laboratory, Malmö University Hospital, Malmö, Sweden); a mouse monoclonal anti-FLT3 sc-19635, anti-STAT1 α (SC 417), and anti-STAT1 α/β (SC 346) were purchased from Santa Cruz Biotechnology (Heidelberg, Germany). Anti-phosphotyrosine mAb 4G10 was from Upstate (Lake Placid, NY). Anti-P-Akt (Ser473) (193H12), anti-Akt (no. 9272), anti-p44/42 MAPK (Thr202/Tyr204, E10; no. 9106), anti-P-Stat1 (Tyr701; no. 9171), anti-P-Stat3 (Tyr705; no. 9131), anti-STAT3 (124H6; no. 9139), anti-P-Stat5 (Y694, EPITOMICS no. 1208-1), and anti-STAT5 (no. 9310) were from Cell Signaling Technology (Frankfurt, Germany). Anti-Erk1 (no. M12320) was purchased from BD Transduction Laboratories (Heidelberg, Germany).

For immunocytochemistry, the FLT3 antibody was purchased from R&D Systems (Minneapolis, MN). The calnexin antibodies and Cy3-conjugated anti-mouse IgG antibodies were purchased from Sigma-Aldrich (St Louis, MO). Alexa Fluor 488-conjugated anti-rabbit IgG was purchased from Molecular Probes (Eugene, OR). For fluorescence-activated cell sorting (FACS) analysis, R-phycoerythrin (R-PE)-conjugated mouse monoclonal anti-FLT3 (BD, Heidelberg, Germany; catalog no. 558996) was used.

Cloning of FLT3 variants

Constructs for human FLT3 wild-type in the vector pAL (kindly provided by Drs Choudhary and Serve, Department of Medicine, Hematology/Oncology, University of Münster, Münster, Germany), and for HA-tagged human FLT3 wild-type, and FLT3 ITD in pcDNA3.1, respectively, have been described earlier.^{16,18}

The R931A mutation, and the K932A, R933A mutations were generated in FLT3 wild-type (HA), and FLT3 ITD (HA) in pcDNA3.1 using the QuikChange Site-Directed Mutagenesis Kit (Stratagene Europe, Amsterdam, The Netherlands) according to the instructions of the manufacturer, using the mutagenesis forward primers 5'-GCTTTTGGACTCAGC-GAAACGGCCATCCTTCC-3', or 5'-CTTTTGGACTCAAGGGCGGCGCC-ATCCTTCC-3', and their complementary reverse counterparts. The RRR (R3) tag was discovered in constructs generated by fusing sequences of human FK506-binding protein 12 to the C-terminus of FLT3. In some of these constructs, shifts of the reading frame occurred, leading to fusion proteins with intracellular retention. The initial constructs contained human FLT wild-type cDNA in pcDNA3.1 with the stop codon replaced with the sequence 5'-GGAGTGCAGGTGGCAGGTGCGAAGATTCGATAGTGC-AGGTGGAGA-CTATCTCCCCAGGAGACGGGCGCACCTTCCCCA-AGCGCGCCAGACCTGCGTGGTGCACTACACCGGGATGCTTGA. The such modified FLT3 was subcloned into FLT3 wild-type or the kinase inactive FLT3 K644A in pAL background using *NdeI/BamHI* restriction and insertion. Generation of the corresponding AAA (A3) control constructs was done with the QuikChange Site Directed Mutagenesis Kit (Stratagene Europe) using the forward primer 5'-GACTATC-TCCCCGCG-GCAGCGGCGCAC-CTTCCC-3' and its corresponding reverse and complementary counterpart. A blasticidine resistance cassette, preceded by an IRES-sequence, was inserted into the pAL-based constructs using *BamHI/BglII* restriction of recipient vector and *BglIII/XbaI* restriction of the donor vector pMSCV-IRES/Bsd (J.P.M., unpublished data, December 2006). The D835Y mutation was generated in FLT3 A3, and FLT3 R3 in the pAL background using the QuikChange Site-Directed Mutagenesis Kit (Stratagene Europe) according to the instructions of the manufacturer using the mutagenesis forward primer 5'-CTTTGGATTGGCTCGATATATCAT-GAGTGATTCC-3' and its complementary reverse counterpart. FLT3 ITD A3, and FLT3 ITD R3 in pAL were generated by replacing sequence in wild-type FLT3 A3 or FLT3 R3 DNA, respectively, with ITD-encoding sequence using the flanking unique restriction sites *MfeI* and *NdeI*.

Cell culture and transfections

HEK293 cells were kept in DMEM/Ham F12 medium (1:1), supplemented with 10% fetal bovine serum (FBS; Biochrom, Berlin, Germany) and antibiotics. For transient transfections, polyethyleneimine (PEI; Aldrich, Deisenhofen, Germany; catalog no. 40872-7) was used at a ratio of 1 μ g DNA to 2.5 μ g PEI. 32Dcl3 cells were kept in RPMI 1640 medium containing 20 mM HEPES, supplemented with 10% heat-inactivated FBS (BioWest, Essen, Germany), 1 mM sodium pyruvate, and 2.5 ng/mL mrecIL-3 (PeproTech, London, United Kingdom). For transfection, 6 to 9 $\times 10^6$ cells were mixed with 20 μ g DNA in 300 μ L culture medium in 0.4-cm gap cuvettes and were electroporated using a pulse of 300 V and 960 μ F, with resistance set to indefinite. After 2 days, selection was started with 15 μ g blasticidine/mL for at least 14 days. All data are representative for several independently selected cell pools. Immortalized mouse embryo fibroblasts with inactivated PTP1B gene (PTP1B^{-/-}) and corresponding cells with rescued PTP1B expression by stable transfection (PTP1B WT) have been described earlier¹⁹ and were kindly provided by Drs Haj and Neel (Harvard University, Boston, MA). They were grown in DMEM with 10% newborn calf serum and transfected with Lipfectamine 2000 (Invitrogen, Karlsruhe, Germany), according to the instructions of the manufacturer.

FACS analysis

For quantification of surface-exposed FLT3, the corresponding 32D cells were washed with PBS and stained with R-PE-labeled anti-FLT3 antibody (10 μ L/10⁶ cells) by incubating in 250 μ L PBS at 4°C for 30 minutes, followed by 2 washes with PBS. For determination of total FLT3, 32D cells were washed once with PBS and subsequently fixed and permeabilized using ice-cold BD Cytotfix/Cytoperm solution (BD, Heidelberg, Germany) for 20 minutes. Subsequently, the cells were resuspended in BD Perm/Wash buffer and stained with R-PE-labeled anti-FLT3 antibody diluted in the same buffer (10 μ L/10⁶ cells) for 30 minutes on ice, followed by 2 washes with BD Perm/Wash buffer. Cells were analyzed with a FACS Canto cytometer (Becton Dickinson, Heidelberg, Germany) using FloJo software (BD Biosciences, Palo Alto, CA).

Immunocytochemical analysis of FLT3 in 32D cells

Immunofluorescence labeling was performed according to standard procedures as previously described.²⁰ In brief, the plasma membrane of 32D cells was stained on ice with WGA conjugated to Alexa Fluor 488 (Molecular Probes); thereafter, cells were fixed with paraformaldehyde, quenched with ammonium chloride, and permeabilized with Triton X-100. Unspecific staining was blocked with FCS. Cells were incubated for 1 hour at room temperature with primary antibodies, washed in PBS, and stained for 1 hour in the dark with fluorophore-conjugated secondary antibodies. The slides were mounted in AntiFade Gold (Molecular Probes). Cells were examined on a confocal Olympus FV 1000 microscope (Olympus, Hamburg, Germany) with a PlanApo 60 \times /1.4 NA oil objective, or a 60 \times /1.35 NA oil objective operating in the sequential acquisition mode with 488/FITC and 561 excitation lasers. Fluorescent images were collected using Olympus FV 10-ASW version 1.6 software and processed using Adobe Photoshop version 7.0.1 (Adobe Systems, San Jose, CA).

Signaling analysis

32D cells and HEK293 cells were either washed once with PBS and lysed directly, or 32D cells were starved from growth factors by incubation in serum- and cytokine-free RPMI 1640 with 1 mM sodium pyruvate, for 4 to 5 hours, followed by lysis or by stimulation with 100 ng/mL FLT3 ligand (FL) at 37°C for 10 minutes before lysis. For FLT3 immunoprecipitation, lysis was done in 1% NP40, 20 mM HEPES, pH 7.4, 0.15 M NaCl, 2 mM EDTA, and 1 mM EGTA. For detection of activated signaling proteins in cell lysates, RIPA buffer containing 1% NP40, 0.25% deoxycholate, 50 mM Tris pH 7.4, 0.15 M NaCl, and 1 mM EDTA was used. Lysis buffers were freshly supplemented with proteinase inhibitors and phosphatase inhibitors (25 mM NaF, 1 mM sodium orthovanadate, and PhosphSTOP; Roche, Mannheim, Germany), and lysis was allowed on ice for 15 minutes, before thorough vortexing and centrifugation. FLT3 immunoprecipitations were

performed by incubating at 4°C overnight with anti-FLT3 antibodies, followed by incubation with Protein A- or Protein G-Sepharose beads. Mouse embryo fibroblasts were seeded in 6-well plates (80 000 cells/well), transfected with FLT3 constructs in pAL on the next day, and subjected to extraction and FLT3 immunoprecipitation after another 48 hours.

Proliferation and colony-forming assays

The proliferation of 32D parental cells and cell lines carrying different FLT3 variants in the absence or presence of FL (10 ng/mL) or IL-3 (2.5 ng/mL) was determined using the 3-(4, 5-dimethylthiazolyl-2)-2, 5-diphenyltetrazolium bromide (MTT) assay.²¹ After washing cells twice with PBS, 2.5×10^4 cells in 100 μ L 3 RPMI 1640 medium containing 10% heat-inactivated FBS, and 1 mM sodium pyruvate, were seeded into 96-well microtiter plates and incubated at 37°C, 5% CO₂ for 48 or 72 hours. Thereafter, 10 μ L MTT solution (5 mg/mL in PBS) was added, and the cells were incubated for another 4 hours. Solubilization reagent (100 μ L; 10% SDS, 0.01 M HCl) was then added, and absorption at 570 nm was measured using a microplate reader. The diagrams represent mean values of 8 parallel samples. Wortmannin was from Aldrich (Deisenhofen, Germany); UO126 and diphenylene iodonium (DPI) were purchased from Axxora (Grünberg, Germany).

The colony-forming cell assays were performed in methylcellulose-solidified Iscove modified Dulbecco medium (IMDM; Invitrogen, Heidelberg, Germany), as described earlier.⁴ In brief, after washing cells twice in serum-free IMDM, 3×10^4 cells were seeded in 1 mL IMDM containing 1% methylcellulose and 20% heat-inactivated FCS without or with the addition of FL (20 ng/mL) and IL-3 (2.5 ng/mL) in 12-well plates (Greiner BIO-ONE, Essen, Germany) in triplicates. The plates were incubated at 37°C, 5% CO₂ for 12 days with intermediate recording after 6 days. Representative sections of the wells were photographed using an Olympus CKX41 microscope equipped with a CAMEDIA C-7070 camera (Olympus Deutschland, Hamburg, Germany).

Animal experiments

Eight- to 10-week-old male C3H/HeJ mice, which are syngeneic to 32Dcl3 cells, were used to assess the *in vivo* development of leukemia-like disease.⁴ 32D cells expressing the different FLT3 variants (2×10^6 each) were injected into the lateral tail vein. Moribund animals were killed by decapitation. The experimental protocols were reviewed and approved by the Committee on Animal Experimentation at the Friedrich Schiller University Jena. For histologic evaluation, murine tissues were fixed for at least 72 hours in 5% neutral buffered formalin (Fischer, Saarbrücken, Germany), dehydrated in alcohol, cleared in xylene, and infiltrated with paraffin on an automated processor.

Results

Identification of a novel ER-targeting sequence

ER retention of transmembrane proteins can be mediated by different types of signal sequences. C-terminal KKXX motifs are critical for retention of different ER resident proteins such as the ER chaperone calnexin. Recognition by the coat protein complex I mediates their retrieval into the ER.²² Internal RxR motifs can also mediate ER retention by yet not well-understood mechanisms. They are, for example, critical for regulated ER retention in the processing of multimeric surface proteins such as ion channels. Preformation of the multimers in the proper stoichiometry in the ER membrane leads to masking of the RxR motifs and allows further processing and surface expression.²³

We have initially explored the possibility that an internal RxR motif in the FLT3 sequence may be exposed in FLT3 ITD, leading to ER retention. If so, mutation of the sequence should allow more efficient surface expression. Indeed, a candidate sequence

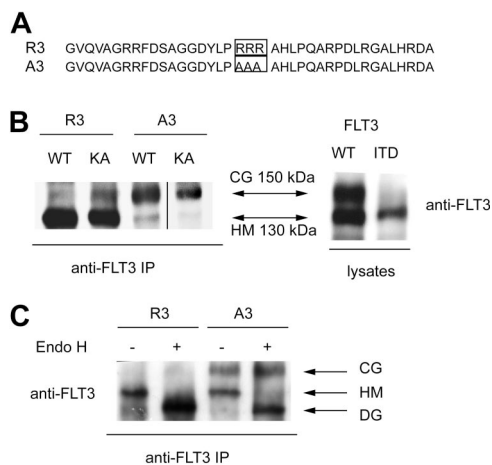


Figure 1. A C-terminal ER-targeting sequence promotes formation of an immature FLT3 receptor. (A) C-terminal sequence that confers FLT3 ER retention (designated R3), and corresponding control sequence that allows normal maturation, designated A3, are depicted. (B) HEK293 cells were transiently transfected with expression constructs for the indicated FLT3 versions and cell lysates were either directly or after FLT3 immunoprecipitation subjected to immunoblotting. R3 indicates FLT3 wild-type with the C-terminal ER retention sequence; A3, FLT3 wild-type with the corresponding control sequence, constructs in vector pAL; FLT3 WT, FLT3-ITD, constructs in pcDNA3. KA indicates the kinase-inactive K644A mutant. A vertical line has been inserted to indicate a repositioned gel lane. (C) 32D cells were stably transfected with FLT3 R3 or FLT3 A3. Cell extracts were subjected to immunoprecipitation, and the precipitates were digested with Endoglycosidase H (EndoH) or subjected to a corresponding mock treatment, as indicated, before sodium dodecyl sulfate–polyacrylamide gel electrophoresis (SDS-PAGE) and immunoblotting. CG indicates complex glycosylated; HM, high-mannose; and DG, deglycosylated forms.

R₉₃₁K₉₃₂R₉₃₃ exists in the FLT3 sequence and, by structural considerations, may be more exposed when the juxtamembrane-kinase interaction is disrupted by the ITD mutation. However, mutation of this sequence in FLT3 ITD led either to an inactive kinase version (K932A, R933A), which matured more efficiently (as all kinase-inactivated mutants do¹⁶), or did not affect maturation (R931A; data not shown).

To achieve deliberate ER anchoring of FLT3, we initially tested the C-terminal fusion of the sequence KKAA. This led only to weak retarding effects on maturation, which could be overridden by kinase-inactivating mutations (not shown). In the process of construction of these and further fusion proteins, a C-terminal extension of FLT3 was generated (see details in “Cloning of FLT3 variants”) that contained an RRR motif embedded in a sequence of an additional 36 amino acids (Figure 1A). Fusion of this sequence (designated R3) to FLT3 led to the preferred formation of a 130-kDa form of the receptor. It corresponds in size to the underglycosylated, ER-bound immature form, which is also enriched for FLT3 ITD (Figure 1B). Replacement of the RRR sequence by AAA (designated A3) resulted in efficient formation of the 150-kDa form, suggesting normal maturation. Importantly, introduction of the kinase-inactivating mutation K644A into R3 did not significantly alter the expression pattern, suggesting that this C-terminal localization signal is dominant over alterations brought about by receptor autophosphorylation (Figure 1B). Fusion of FLT3 to an N-terminally truncated version of the R3 targeting sequence, which was 16 amino acids shorter, still resulted in formation of largely immature FLT3, whereas directly appending only the sequence RRR to the C-terminus had no effect on the maturation pattern (data not shown). Expression of FLT3 R3 in 32D cells gave, as in HEK293 cells, rise to almost exclusively the 130-kDa form, whereas FLT3 A3 expressed similar amounts of the 130- and the 150-kDa forms. Digestion of corresponding

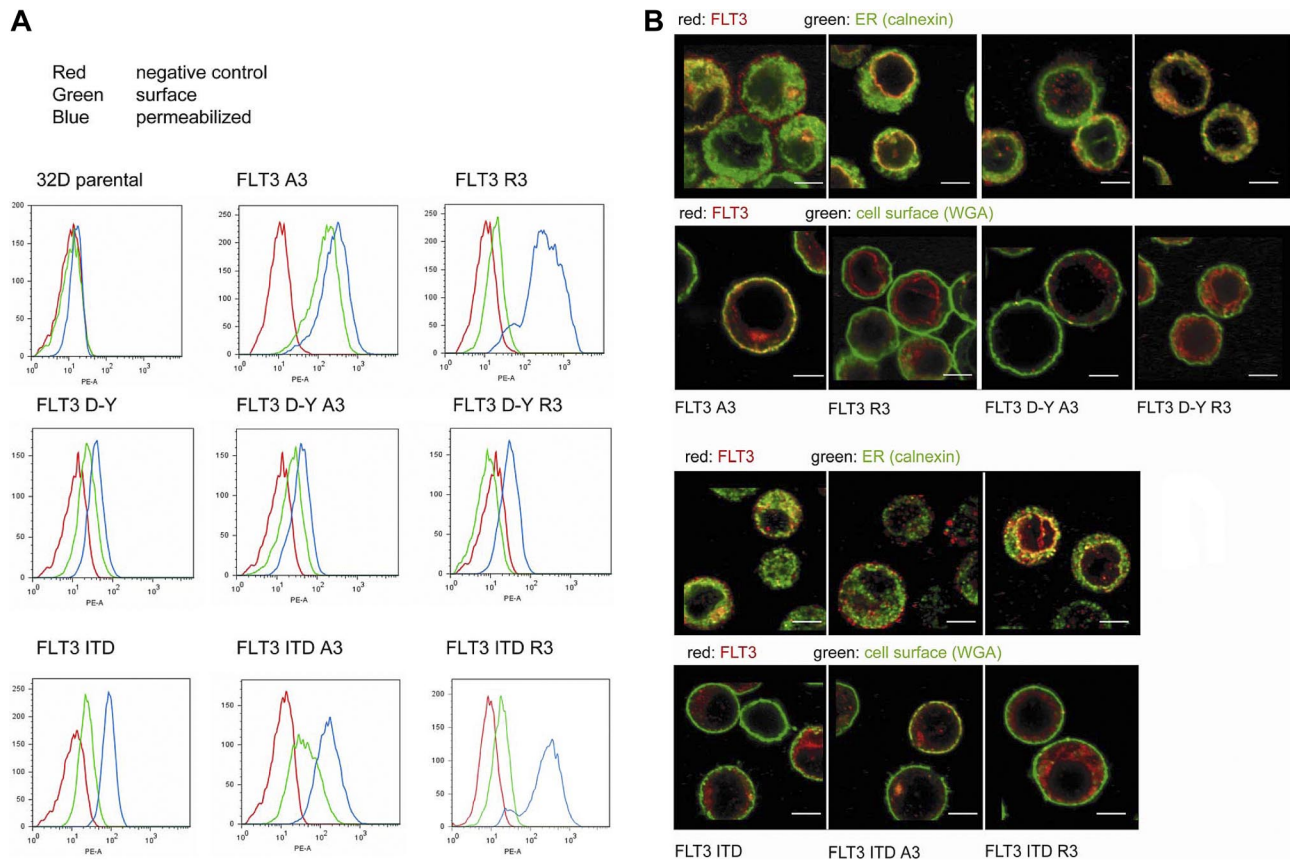


Figure 2. Intracellular retention of ER-targeted FLT3. (A) 32D cells expressing FLT3 A3, or FLT3 R3, FLT3 D835Y, FLT3 D835Y R3, or FLT3 D835Y A3, FLT3 ITD, FLT3 ITD A3, or FLT3 ITD R3, as indicated, were subjected to FACS analysis using PE-labeled anti-FLT3 antibodies. The analysis was performed without or with prior cell permeabilization. Parental 32D cells were analyzed in parallel as negative controls for all series (red curves). An example analysis is shown (top left). (B) Cellular localization of FLT3 A3 or FLT3 R3, FLT3 D835Y R3, or FLT3 D835Y A3, FLT3 ITD, FLT3 ITD A3, or FLT3 ITD R3 (as indicated) shown by immunofluorescence using confocal laser scanning microscopy using equipment described in "Immunocytochemical analysis of FLT3 in 32D cells." Counterstaining of the cells was performed with an antibody against the ER-resident protein calnexin or with fluorescently labeled wheat-germ agglutinin to mark the cell surface, as indicated. Scale bars correspond to 5 μ m.

immunoprecipitates with endoglycosidase H (EndoH) led to loss of the 130-kDa form of both FLT3 R3 and FLT3 A3 and formation of an approximately 110-kDa product (Figure 1C) known to represent deglycosylated FLT3.^{16,24} EndoH sensitivity indicated that the 130-kDa form, which is prevalent in FLT3 R3, contains high-mannose carbohydrates, which are typical for immature ER resident glycoproteins. FACS analysis of FLT3 A3-expressing 32D cells showed the presence of receptors at the cells surface, whereas little if any receptor was detectable at the surface in the case of FLT3 R3. The latter species became, however, abundantly detectable on permeabilization of the cells, indicating that an intracellular localization prevented detection in the nonpermeabilized cells (Figure 2A). Similar data were obtained for cell lines stably transfected with expression constructs for the constitutively active FLT3 D835Y R3 and FLT3 D835Y A3 and for the FLT3 ITD R3 and A3 versions, except that the corresponding cell lines expressed in part lesser amounts of receptor. FLT3 ITD R3 expression levels were obviously somewhat more variable, resulting in a broader distribution of signal intensity in the FACS analysis (Figure 2A). To further establish the differential localization of the tagged FLT3 versions, the stably transfected 32D cell lines were subjected to confocal immunofluorescence microscopy. As shown in Figure 2B, wild-type FLT3 R3 was largely detectable in a perinuclear compartment, partially colocalizing with the ER marker calnexin. In sharp contrast, FLT3 A3 was virtually absent from this compartment of the ER. Consistent with the FACS data, it was prominently detectable in the plasma membrane at least in a fraction of cells. An

intracellular fraction of FLT3 A3 was, however, also detectable, presumably representing the minor band of the high-mannose species shown by the biochemical analysis. Differently from FLT3 R3, this pool of FLT3 A3 was localized in more peripheral membranes, which have not yet been identified and could represent ER or, potentially, Golgi vesicles (Figure 2B). A similar localization could be detected for the corresponding FLT3 D835Y versions (Figure 2B), although lower expression levels of these receptor variants partially compromised the quality of the images. As described earlier,^{16,20} FLT3 ITD was detectable intracellularly, and a fraction was also detectable at the cell surface (Figure 2B). Attachment of the R3 tag removed the surface-bound receptor and led to enrichment in a perinuclear, calnexin-positive compartment (Figure 2B). In contrast, FLT3 ITD A3 was not further enriched intracellularly, compared with the untagged FLT3 ITD. In contrast, the A3 tag seemed to even promote somewhat a surface localization (Figure 2B).

Taken together, by attaching the R3 sequence to the C-terminus, FLT3 and activated FLT3 mutants can be anchored in a perinuclear compartment of the ER, whereas attachment of the mutated A3 control sequence allows normal processing of FLT3, maturation into a complex glycosylated form, and expression at the cell surface.

Signaling properties of ER-bound wild-type FLT3 and FLT3 D835Y

32D cells stably expressing the different FLT3 variants were subjected to a comparative analysis of signal transduction. The

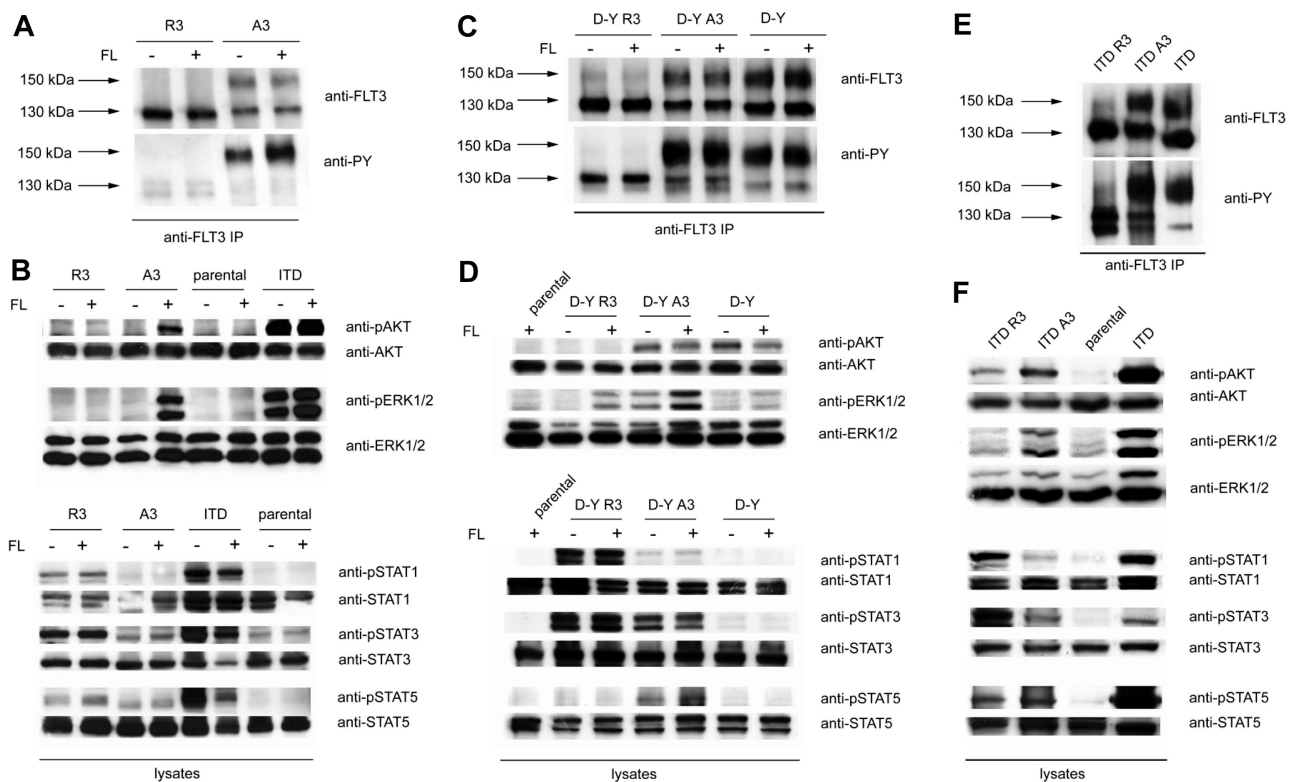


Figure 3. Different signaling quality of ER-bound and surface FLT3. (A) 32D cells expressing FLT3 R3 or FLT3 A3 were starved and stimulated with FL (100 ng/mL, 10 minutes) or left unstimulated, as indicated. FLT3 was immunoprecipitated and analyzed by immunoblotting with anti-FLT3 or anti-phosphotyrosine antibodies (4G10). (B) 32D cells expressing FLT3 R3, FLT3 A3, or FLT3 ITD, as well as parental 32D cells, were starved and stimulated with FL (100 ng/mL, 10 minutes) or left unstimulated, as indicated. Lysate aliquots were subjected to analysis of phosphorylated signaling proteins and of the corresponding proteins for loading controls, as indicated. (C) 32D cells expressing FLT3 D835Y R3 or FLT3 D835Y A3 were starved and stimulated with FL (100 ng/mL, 10 minutes) or left unstimulated, as indicated. FLT3 was immunoprecipitated and analyzed by immunoblotting with anti-FLT3 or anti-phosphotyrosine antibodies (4G10). (D) Signal transduction of FLT3 D835Y R3- and FLT3 D835Y A3-expressing cells was analyzed as described in panel B. (E) 32D cells expressing FLT3 ITD, FLT3 ITD R3, or FLT3 ITD A3 were starved, and FLT3 was immunoprecipitated and analyzed by immunoblotting with anti-FLT3 or anti-phosphotyrosine antibodies (4G10). (F) Constitutive signal transduction of FLT3 D835Y ITD, FLT3 ITD A3, and FLT3 ITD R3 was analyzed by immunoblotting in lysates of starved cells.

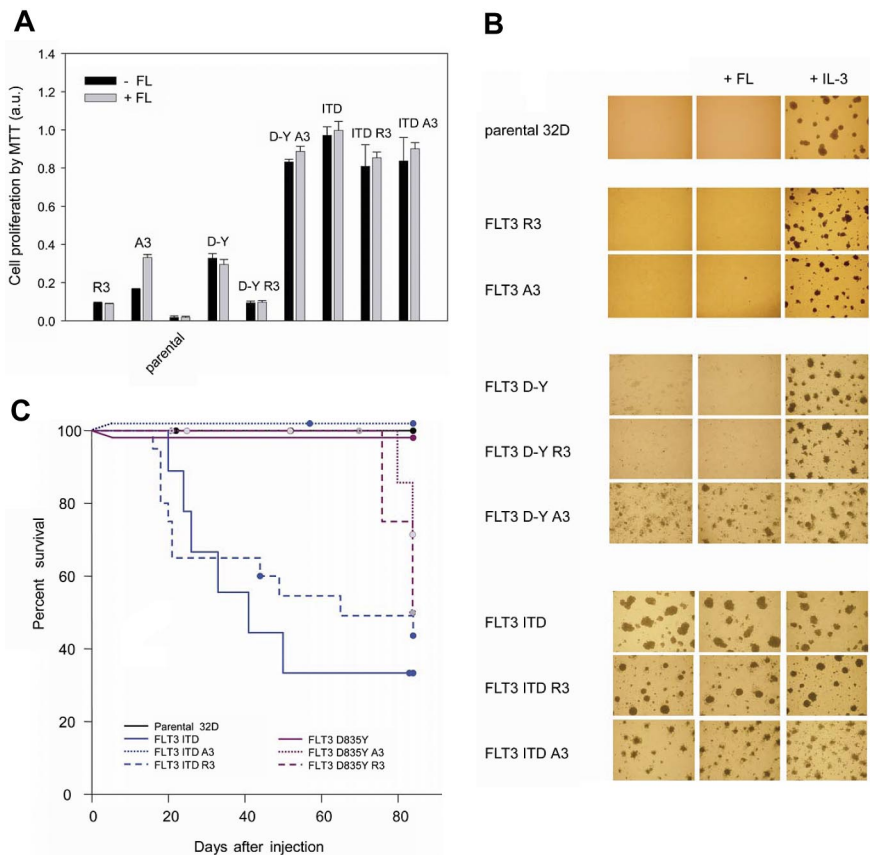
expression pattern of the wild-type FLT3 variants was consistent with the pattern in HEK293 cells. In the case of FLT3 R3, only the 130-kDa form was formed, whereas FLT3 A3-transfected cells expressed similar amounts of 150- and 130-kDa forms (Figure 3A). FLT3 A3 displayed a certain level of constitutive autophosphorylation of the complex glycosylated form, possibly caused by the C-terminal tag, which could, however, readily be enhanced by stimulation with FL (Figure 3A). Further, FLT3 A3 mediated FL-dependent ERK1/2 and AKT activation (Figure 3B). Autophosphorylation of FLT3 A3 and proper ligand response indicated that the C-terminal tag does not grossly interfere with receptor function. In contrast, FLT3 R3 exhibited only a low level of tyrosine phosphorylation. Autophosphorylation and downstream signaling of FLT3 R3 could not be enhanced by stimulation with FL (Figure 3A,B), consistent with inaccessibility of FLT3 R3 by the ligand because of the intracellular localization. Interestingly, ER anchoring of FLT3 led to constitutive activation of STAT1 and STAT3 (Figure 3B). This effect could be suppressed by the FLT3 kinase inhibitor PKC412, suggesting that FLT3 kinase activity was required (Figure S1, available on the *Blood* website; see the Supplemental Materials link at the top of the online article). Stimulation of parental 32D cells did not result in any of the above-mentioned signaling events, indicating that expression of endogenous FLT3, if any, is negligible.

FLT3 D835Y A3, as well as untagged FLT3 D835Y, exhibited constitutive autophosphorylation, which under the tested conditions was not enhanced further by FL stimulation. Phosphorylation

of the 150-kDa mature form was strongly preferred, compared with the immature form. FLT3 D835Y R3 displayed only a relatively low level of constitutive phosphorylation. It appears that the ER retention quenches the autophosphorylation (Figure 3C). We considered the possibility that this may be caused by protein-tyrosine phosphatases (PTPs) that suppress overall phosphorylation of FLT3 in the ER compartment. A candidate PTP could be PTP1B, which is anchored in the ER,²⁵ and can dephosphorylate FLT3 effectively.^{16,26} To test this possibility, we expressed ER-anchored FLT3 D835Y R3 in PTP1B-deficient fibroblasts. The immature state of FLT3 was maintained in these cells, because only the 130-kDa receptor was detectable. However, FLT3 D835Y R3 exhibited a strong autophosphorylation in these cells, as opposed to expression in fibroblasts harboring wild-type PTP1B (Figure S2). Expression in PTP1B-deficient fibroblasts resulted also in autophosphorylation of wild-type FLT3 R3. Furthermore, when untagged FLT3 or FLT3 D835Y was expressed in these cells, the phosphorylation of the immature form of these receptor variants, but not of the complex glycosylated form, was likewise greatly enhanced (Figure S2). These data do not only indicate the relevance of ER-associated PTP activity but are also in support of normal dimerization and autokinase activity of ER-anchored FLT3 variants.

FLT3 D835Y exhibited constitutive AKT and ERK1/2 activation, and the latter could be further enhanced by FL stimulation (Figure 3D). Constitutive and ligand-induced ERK1/2 activation were elevated in FLT3 D835Y A3, indicating some additional activation of this FLT3 variant by the C-terminal tag. In addition,

Figure 4. Growth and transforming capacity of 32D cell lines expressing ER-targeted FLT3. (A) 32D cell lines expressing the indicated FLT3 variants or parental 32D cells were seeded in 96-well plates (2.5×10^4 cells/well), and cell growth in the absence or presence of FL (10 ng/mL) or IL-3 (2.5 ng/mL) was measured after 2 days using the MTT method. Values were normalized to growth in the presence of IL-3, which was set to 1.0 (means \pm SD, $n = 8$). (B) The indicated versions of 32D cell pools were subjected to colony formation assays in methylcellulose in the absence or presence of FL or IL-3. Representative sections were photographed after 5 to 6 days of culture using equipment described in "Proliferation and colony-forming assays." (C) Kaplan-Meier plot of survival of C3H/HeJ mice receiving parental 32D cells or 32D cells expressing the different FLT3 versions as indicated. Each group contained 8 to 10 mice. The percentage of surviving mice (y-axis) is plotted with respect to time in days (x-axis). Circles represent mice killed without a myeloproliferative disease or which served as controls at various time points, respectively. Statistical significance was tested using Gehan-Breslow statistics for the survival curves; post hoc comparisons were made with the Holm-Sidak method for all pairwise multiple comparisons. The reduction of survival in case of application of FLT3 ITD or FLT3 ITD R3-expressing cells was significant ($P < .05$) compared with all other groups. There was no statistical difference in survival between parental cells and any of the FLT3 D835Y-harboring cells, nor among the latter.



FLT3 D835Y A3 expression led to weak STAT5 and clear STAT3 activation which was absent in the case of FLT3 D835Y. Given the higher basal activity of the A3-tagged FLT3 D835Y, the abolishment of constitutive ERK1/2 and AKT activity in case of the ER-anchored FLT3 D835Y R3 variant was remarkable (Figure 3D). We observed a weak FL-dependent ERK1/2 activation, which is presumably caused by a minor fraction of surface-accessible receptor. ER anchoring of FLT3 D835Y promoted STAT1 and STAT3 activation, which was clearly more pronounced than in the case of wild-type FLT3 R3.

Signaling properties of ER-bound FLT3 ITD

FLT3 ITD occurred predominantly in the immature form (Figure 3E), consistent with earlier observations,¹⁶ and with the localization data (Figure 2A,B). Tyrosine phosphorylation was, however, predominant in the mature receptor. Similarly, for FLT3 ITD A3 efficient constitutive tyrosine phosphorylation of the mature form was readily detectable. In the case of FLT3 ITD R3, the immature form was even more predominant. Notably, nearly no tyrosine phosphorylated 150-kDa form could be seen, in contrast to untagged or A3-tagged receptor. FLT3 ITD R3 autophosphorylation was readily detectable. Antiphosphotyrosine detection showed 2 bands with slightly different mobility, whose origin is currently unknown. Expression of FLT3 ITD R3 in PTP1B-negative fibroblasts enhanced autophosphorylation. This applied also to the immature form of the untagged FLT3 ITD (Figure S2). These findings indicate that also FLT3 ITD autophosphorylation is under negative control by this PTP in the ER.

FLT3 ITD triggered abundant constitutive activation of ERK1/2 and AKT. Similarly, FLT3 ITD A3 caused constitutive ERK1/2 and AKT signaling, albeit at lower levels as FLT3 ITD. In the case of FLT3 ITD R3, constitutive ERK1/2 activation was abrogated, and

AKT activation was reduced (Figure 3F). However, STAT5 activation was still readily detectable for FLT3 ITD R3, and it reached similar levels as for the corresponding FLT3 ITD A3. Further, STAT1 and STAT3 activation by FLT3 ITD R3 was robust and obviously enhanced compared with FLT3 ITD and FLT3 ITD A3.

Effects of FLT3 ER targeting on growth and transformation

We also addressed whether the ER-targeted FLT3 would affect growth and potentially colony formation of corresponding 32D cell lines. As shown in Figure 4A, neither FLT3 R3 nor FLT3 A3 were capable of sustaining cytokine-independent growth. In the presence of FL, FLT3 A3-expressing cells could, however, be stimulated to grow, consistent with the surface localization of FLT3 A3, and as expected for wild-type FLT3.⁴ FLT3 D835Y-expressing cells exhibited a moderate growth in the absence and presence of FL. Consistent with elevated signal transduction of this variant, FLT3 D835Y A3 led to a pronounced cytokine-independent growth, again indicating an activating effect of the C-terminal tag on this receptor mutant. In an attempt to characterize the underlying signaling pathways for this effect, we compared different signal transduction inhibitors. Wortmannin and UO126 were used to test the role of PI3-kinase/AKT activation and MEK/ERK activation, respectively. To explore the possible role of STAT5 activation, we used DPI, a general NADPH-oxidase inhibitor. It has recently been shown that STAT5 activation promotes generation of reactive oxygen species, which is presumably important for the transformation process.²⁷ The obtained data suggest that growth of untagged FLT3 D835Y-expressing cells depends on AKT and MEK/ERK activation, whereas STAT5 and to a lesser extent MEK/ERK are important for growth of FLT3 D835Y A3-expressing cells (Figure S3). ER anchoring of the tagged receptor by using the R3 motif in the C-terminal tag, however, completely abrogated growth.

Table 1. Signaling of FLT3 mutant proteins and effect of ER targeting

	Autophosphorylation		Activation				Proliferation	Colony formation	MPD formation
	130 kDa	150 kDa	STAT5	STAT3	ERK1/2	AKT			
FLT3 D835Y	+	+++	–	–	(+)	+	+	–	–
FLT3 D835Y R3	+	–	–	++	–	–	–	–	–
FLT3 ITD	+	+++	+++	+	++	++	++	+++	++
FLT3 ITD R3	++	–	++	++	(+)	+	++	++	+

FLT3 ITD supported robust cytokine-independent growth, which was similar also in the case of the FLT3 ITD A3 and R3 versions (Figure 4A). Thus, ER-anchored FLT3 ITD R3 is still mitogenic and differs substantially from ER-anchored FLT3 D835Y R3. Similar results were obtained by testing clonogenic growth in methylcellulose (Figure 4B). Cells expressing FLT3 A3, FLT3 R3, or FLT3 D835Y did not form colonies in the absence of IL-3. In contrast, the FLT3 D835Y A3-expressing cells were capable of forming colonies. FLT3 D835Y R3-expressing cells were again unable to grow. FLT3 ITD readily formed colonies in the absence of cytokines. FLT3 ITD A3 and R3 likewise sustained colony growth; however, growth was in both cases somewhat delayed and became apparent by inspection at earlier time points (data not shown).

In C3H/HeJ mice, injection of FLT3 ITD-expressing cells led to a fatal MPD (Figure 4C), although efficiency of tumor formation was reduced compared with 32D cells expressing an ITD mutant in a murine FLT3 context⁴ (data not shown). Surprisingly, the FLT3 ITD A3-expressing cells did not grow in mice. Cells harboring the FLT3 D835Y versions caused MPD only in rare cases at late time points, even in the case of FLT3 D835Y A3. Importantly, FLT3 ITD R3 caused MPD in a significant fraction of the mice, further supporting that FLT3 ITD at least partially retains transforming capacity when anchored in the ER.

Discussion

As shown in this study, FLT3 could be engineered to remain in an intracellular localization in the perinuclear ER by C-terminal attachment of a novel targeting sequence that contains a R3 motif. Maintaining the embedding sequence and mutating the critical 3 arginine residues in this tag to 3 alanines (A3), led to loss of the ER-targeting function and to normal maturation of the A3-tagged receptor variants. The targeting sequence contains 39 amino acids. The minimal sequence requirements for ER retention remain to be characterized. The novel targeting strategy may potentially be more generally applicable, i.e., to other receptor tyrosine kinases. It allowed us to test effects of the different cellular localization on FLT3 signaling.

Not surprisingly, ER-anchoring of wild-type FLT3 led to loss of ligand responsiveness in terms of autophosphorylation and of concomitant activation of ERK1/2 and AKT. Intracellular localization of FLT3 R3 obviously prevents access of the ligand. Furthermore, ER anchoring does not lead to spontaneous activation, apart from a weak activation of STAT3. Ligand responses were, however, readily detectable with the FLT3 A3 control variant. Normal functionality of FLT3 A3 indicated that attachment of the C-terminal tag did not grossly interfere with basal functions of FLT3 such as ligand binding, dimerization, and autokinase activity. In case of the constitutively active FLT3 mutant D835Y, C-terminal tagging with the A3-containing sequence even enhanced basal receptor activity compared with the untagged FLT3 D835Y variant, which translated into elevated ERK1/2 and AKT activation, weak activation of STAT5, cytokine independent growth, and colony

formation in semisolid medium. Routing of the tagged receptor into the ER using the RRR motif, strongly suppressed all these responses, reducing signaling to a level even clearly below that of the untagged FLT3 D835Y. However, expressing the ER-targeted FLT3 D835Y R3 in PTP1B-deficient fibroblasts restored robust autophosphorylation, in contrast to expression in PTP1B-expressing control cells. Elevated autophosphorylation of ER-targeted or the immature forms, respectively, was also found for wild-type FLT3 and for FLT3 ITD in PTP1B-deficient cells. These findings indicate that the ER environment is inhibitory for global receptor autophosphorylation and for certain signaling events, presumably through ER-resident PTPs. PTP1B may indeed be particularly important in this context because it is ER anchored,²⁵ and elevated PTP1B activity has recently been shown in the perinuclear compartment.²⁸ Interestingly, the ER-anchored FLT3 D835Y R3 stimulated pronounced activation of STAT3 and STAT1, indicating that ER-associated inhibition of signaling is selective, and that ER anchoring caused also the acquisition of new signaling qualities. These were, however, in the context of the D835Y mutant receptor, insufficient to translate into cell growth and transformation.

In the case of FLT3 ITD, the untagged receptor was to a significant extent immature and intracellular, and it sustained robust constitutive activation of ERK1/2, AKT, STAT5, and to a lesser extent STAT3 and STAT1. Attachment of the A3 tag partially compromised activity; still the qualitative pattern of signal transduction was similar to the parental receptor, albeit at lower levels. The ER-targeted FLT3 ITD R3 exhibited nearly exclusive intracellular localization. Notably, the formation of a highly phosphorylated, complex glycosylated 150-kDa receptor species, which was apparent for FLT3 ITD and FLT3 ITD A3, was strongly suppressed by the R3-mediated anchoring in the ER. Consistent with the observations in the case of FLT3 D835Y, ER-anchoring reduced constitutive ERK1/2, and to a lesser extent AKT activation. Importantly, FLT3 ITD R3 still activated STAT5, as well as STAT3 and STAT1, and can apparently override a negative regulation by ER-resident PTPs. Again, ER retention of FLT3 ITD appeared to even enhance at least the STAT3 activation.

All FLT3 ITD variants caused cytokine-independent growth and colony formation of 32D cells, although the latter was somewhat less efficient in the case of FLT3 ITD A3 and FLT3 ITD R3, perhaps caused by somewhat lower expression levels. This may also be the reason why FLT3 ITD A3-expressing cells did not give rise to MPD. Importantly, cells expressing the ER-targeted FLT3 ITD R3 were also partially transforming in vivo. It is tempting to speculate that preserved STAT5 activation by this receptor variant, in conjunction with the acquisition of enhanced STAT3 signaling, is sufficient to drive transformation and can compensate for reduced ERK1/2 and AKT activation. The predominance of STAT5 activation for transformation by FLT3 ITD has been indicated by previous studies.^{15,27} STAT3 activation is relatively common in AML, but in most cases the mechanism of activation is unclear,²⁹ as well as its possible role for the disease. An essential role of STAT3 activation downstream of FLT3 has,

however, been shown for dendritic cell differentiation.³⁰ In this setting, STAT3 activation mediates proliferation and synergizes with IL-6.³¹ STAT3 has also been identified as direct transcriptional inducer of vascular endothelial growth factor expression.³² STAT1 activation is believed to mediate antiproliferative effects; however, this depends on the context of other cytokines. Interferon γ had no significant effect on AML blast proliferation in the presence of FL.³³ It is possible that notably STAT3 activation may play a role for pathology under conditions of stimulation with other cytokines or for angiogenesis.

Our findings highlight the relevance of cellular localization of FLT3 for signaling quality (Table 1): (1) ER retention was found associated with reduced global receptor autophosphorylation, and with quenching of ERK1/2, and AKT activation; (2) ER targeting caused elevated STAT3 activation; (3) robust STAT5 activation by FLT3 ITD was retained when formation of mature receptor was abrogated by ER targeting. These observations uncover previously unrecognized aspects of FLT3 ITD signaling and transformation quality.

We propose that exposure of the receptor to ER-resident PTPs, notably PTP1B, may be related to inhibition of autophosphorylation and inactivation of certain signaling events. Maintenance of STAT5 activation by FLT3 ITD R3 and even enhancement of STAT3 activation indicate, however, that the effects of PTP-mediated dephosphorylation should be selective, possibly through selectivity for certain FLT3 autophosphorylation sites. Sites that are less well dephosphorylated by ER-resident PTPs may form the basis for STAT5 activation possibly through direct association. This hypothesis shall be tested in future investigations. The mechanistic basis for enhanced STAT3 activation by ER-anchored FLT3 is currently unclear. Some reports in the literature have likewise indicated that STAT3 activation occurs effectively from intracellular compartments such as endosomes,³⁴ or the ER.³⁵ A differential cellular localization of STAT3 is unlikely to form the basis for this phenomenon, because it appears distributed throughout the cytoplasm.³⁶ Alternatively, one could assume that negative control of STAT3 activation is more pronounced in proximity to the cell surface and less effective in the perinuclear compartment. STAT5 activation, presumably by a direct mechanism,¹⁴ is a hallmark of FLT3 ITD signaling quality and is associated with effective transformation.⁴ Correlating with sustained STAT5 activation, ER-anchored FLT3 ITD is transforming *in vitro* and partially *in vivo*.

The finding that intracellular FLT3 ITD has the capacity to transform cells is a major result of this study.

Acknowledgments

We greatly acknowledge provision of FLT3 cDNA constructs by Chunaram Choudhary and Hubert Serve at the University of Münster, and Frankfurt/Main; of a mFLT3-ITD-expressing 32D cell line by Drs Justus Duyster and Rebekka Grundler at the Technical University of Munich; of PKC412 by Prof Thomas Fischer, University of Mainz; and of anti-FLT3 antibodies by Prof Lars Rönnstrand, University of Malmö-Lund. We also thank Dr Fawaz Haj and Prof Benjamin Neel (Harvard University, Boston, MA) for provision of PTP1B-deficient mouse embryo fibroblasts. We thank Drs. Bülent Sargin, and Lara Tieckenbrock (University of Münster) for help with establishing the 32D cell animal experiments and the colony-formation assays. We thank Rinesh Godfrey for the suggestion to use DPI as an indicator for STAT5 involvement in signaling.

This work was supported by a collaborative grant from Deutsche Krebshilfe (Oncogene Networks in the Pathogenesis of AML).

Authorship

Contribution: D.S.-A. developed the concept and did biochemical experiments; S.-A.B. cloned all constructs, did most biochemical experiments, and performed the signaling analysis; S. Koch and C.T. did the FLT3 immunocytochemistry; J.P.M. did FACS analyses; S.-A.B., L.B., and S. Korasikha did growth and colony assays; H.C. analyzed a putative endogenous ER retention motif; R.B. did the animal experiments; and F.-D.B. coordinated the study and wrote the manuscript.

Conflict-of-interest disclosure: The authors declare no competing financial interests.

Correspondence: F.-D. Böhmer, Institute of Molecular Cell Biology, Center for Molecular Biomedicine, Friedrich Schiller University, Hans-Knöll-Strasse 2, D-07745 Jena, Germany; e-mail boehmer@med.uni-jena.de.

References

- Thiede C, Steudel C, Mohr B, et al. Analysis of FLT3-activating mutations in 979 patients with acute myelogenous leukemia: association with FAB subtypes and identification of subgroups with poor prognosis. *Blood*. 2002;99:4326-4335.
- Nakao M, Yokota S, Iwai T, et al. Internal tandem duplication of the *flt3* gene found in acute myeloid leukemia. *Leukemia*. 1996;10:1911-1918.
- Griffith J, Black J, Faerman C, et al. The structural basis for autoinhibition of FLT3 by the juxtamembrane domain. *Mol Cell*. 2004;13:169-178.
- Mizuki M, Fenski R, Halfter H, et al. FLT3 mutations from patients with acute myeloid leukemia induce transformation of 32D cells mediated by the Ras and STAT5 pathways. *Blood*. 2000;96:3907-3914.
- Kelly LM, Liu Q, Kutok JL, Williams IR, Boulton CL, Gilliland DG. FLT3 internal tandem duplication mutations associated with human acute myeloid leukemias induce myeloproliferative disease in a murine bone marrow transplant model. *Blood*. 2002;99:310-318.
- Grundler R, Miething C, Thiede C, Peschel C, Duyster J. FLT3-ITD and tyrosine kinase domain mutants induce 2 distinct phenotypes in a murine bone marrow transplantation model. *Blood*. 2005;105:4792-4799.
- Small D. FLT3 mutations: biology and treatment. *Hematology Am Soc Hematol Educ Program*. 2006;178-184.
- Reindl C, Bagrintseva K, Vempati S, et al. Point mutations in the juxtamembrane domain of FLT3 define a new class of activating mutations in AML. *Blood*. 2006;107:3700-3707.
- Breitenbuecher F, Schnittger S, Grundler R, et al. Identification of a novel type of ITD mutations located in non-juxtamembrane domains of the FLT3 tyrosine kinase receptor. *Blood*. Prepublished May 15 2008; DOI 10.1182/blood-2007-11-125476.
- Schmidt-Arras D, Schwäble J, Böhmer FD, Serve H. FLT3 receptor tyrosine kinase as a drug target in leukemia. *Curr Pharm Des*. 2004;10:1867-1883.
- Levis M, Small D. FLT3 tyrosine kinase inhibitors. *Int J Hematol*. 2005;82:100-107.
- Müller-Tidow C, Steur C, Mizuki M, et al. [Mutations of growth factor receptor Flt3 in acute myeloid leukemia: transformation of myeloid cells by Ras-dependent and Ras-independent mechanisms]. *Dtsch Med Wochenschr*. 2002;127:2195-2200.
- Choudhary C, Müller-Tidow C, Berdel WE, Serve H. Signal transduction of oncogenic Flt3. *Int J Hematol*. 2005;82:93-99.
- Choudhary C, Brandts C, Schwäble J, et al. Activation mechanisms of STAT5 by oncogenic Flt3-ITD. *Blood*. 2007;110:370-374.
- Murata K, Kumagai H, Kawashima T, et al. Selective cytotoxic mechanism of GTP-14564, a novel tyrosine kinase inhibitor in leukemia cells expressing a constitutively active Fms-like tyrosine kinase 3 (FLT3). *J Biol Chem*. 2003;278:32892-32898.
- Schmidt-Arras DE, Böhmer A, Markova B, Choudhary C, Serve H, Böhmer FD. Tyrosine phosphorylation regulates maturation of receptor tyrosine kinases. *Mol Cell Biol*. 2005;25:3690-3703.
- Xiang X, Kreisel F, Cain J, Colson A, Tomasson MH. Neoplasia driven by mutant c-KIT is mediated by intracellular, not plasma membrane, receptor signaling. *Mol Cell Biol*. 2007;27:267-282.
- Mizuki M, Schwäble J, Steur C, et al. Suppression of myeloid transcription factors and induction

- of STAT response genes by AML-specific Flt3 mutations. *Blood*. 2003;101:3164-3173.
19. Haj FG, Markova B, Klamann LD, Böhmer FD, Neel BG. Regulation of receptor tyrosine kinase signaling by protein tyrosine phosphatase-1B. *J Biol Chem*. 2003;278:739-744.
 20. Koch S, Jacobi A, Ryser M, Ehninger G, Thiede C. Abnormal localization and accumulation of FLT3-ITD, a mutant receptor tyrosine kinase involved in leukemogenesis. *Cells Tissues Organs*. 2008;188:225-235.
 21. Mosmann T. Rapid colorimetric assay for cellular growth and survival: application to proliferation and cytotoxicity assays. *J Immunol Methods*. 1983;65:55-63.
 22. van Vliet C, Thomas EC, Merino-Trigo A, Teasdale RD, Gleeson PA. Intracellular sorting and transport of proteins. *Prog Biophys Mol Biol*. 2003;83:1-45.
 23. Michelsen K, Yuan H, Schwappach B. Hide and run. Arginine-based endoplasmic-reticulum-sorting motifs in the assembly of heteromultimeric membrane proteins. *EMBO Rep*. 2005;6:717-722.
 24. Maroc N, Rottapel R, Rosnet O, et al. Biochemical characterization and analysis of the trans-forming potential of the FLT3/FLK2 receptor tyrosine kinase. *Oncogene*. 1993;8:909-918.
 25. Frangioni JV, Oda A, Smith M, Salzman EW, Neel BG. Calpain-catalyzed cleavage and subcellular relocation of protein phosphotyrosine phosphatase 1B (PTP-1B) in human platelets. *EMBO J*. 1993;12:4843-4856.
 26. Stuible M, Zhao L, Aubry I, et al. Cellular inhibition of protein tyrosine phosphatase 1B by uncharged thioxothiazolidinone derivatives. *Chembiochem*. 2007;8:179-186.
 27. Sallmyr A, Fan J, Datta K, et al. Internal tandem duplication of FLT3 (FLT3/ITD) induces increased ROS production, DNA damage, and misrepair: implications for poor prognosis in AML. *Blood*. 2008;111:3173-3182.
 28. Yudushkin IA, Schleifenbaum A, Kinkhabwala A, Neel BG, Schultz C, Bastiaens PI. Live-cell imaging of enzyme-substrate interaction reveals spatial regulation of PTP1B. *Science*. 2007;315:115-119.
 29. Steensma DP, McClure RF, Karp JE, et al. JAK2 V617F is a rare finding in de novo acute myeloid leukemia, but STAT3 activation is common and remains unexplained. *Leukemia*. 2006;20:971-978.
 30. Laouar Y, Welte T, Fu XY, Flavell RA. STAT3 is required for Flt3L-dependent dendritic cell differentiation. *Immunity*. 2003;19:903-912.
 31. Cohen PA, Koski GK, Czerniecki BJ, et al. STAT3- and STAT5-dependent pathways competitively regulate the pan-differentiation of CD34pos cells into tumor-competent dendritic cells. *Blood*. 2008;112:1832-1843.
 32. Niu G, Wright KL, Huang M, et al. Constitutive Stat3 activity up-regulates VEGF expression and tumor angiogenesis. *Oncogene*. 2002;21:2000-2008.
 33. Ersvaer E, Skavland J, Ulvestad E, Gjertsen BT, Bruserud O. Effects of interferon gamma on native human acute myelogenous leukaemia cells. *Cancer Immunol Immunother*. 2007;56:13-24.
 34. Shah M, Patel K, Mukhopadhyay S, Xu F, Guo G, Sehgal PB. Membrane-associated STAT3 and PY-STAT3 in the cytoplasm. *J Biol Chem*. 2006;281:7302-7308.
 35. Waris G, Tardif KD, Siddiqui A. Endoplasmic reticulum (ER) stress: hepatitis C virus induces an ER-nucleus signal transduction pathway and activates NF-kappaB and STAT-3. *Biochem Pharmacol*. 2002;64:1425-1430.
 36. Pranada AL, Metz S, Herrmann A, Heinrich PC, Müller-Newen G. Real time analysis of STAT3 nucleocytoplasmic shuttling. *J Biol Chem*. 2004;279:15114-15123.